Approximate analytical solutions for excitation and propagation in cardiac tissue

D'Artagnan Greene and Yohannes Shiferaw
Department of Physics and Astronomy, California State University, Northridge, California 91330, USA
(Received 2 January 2015; published 30 April 2015)

It is well known that a variety of cardiac arrhythmias are initiated by a focal excitation in heart tissue. At the single cell level these currents are typically induced by intracellular processes such as spontaneous calcium release (SCR). However, it is not understood how the size and morphology of these focal excitations are related to the electrophysiological properties of cardiac cells. In this paper a detailed physiologically based ionic model is analyzed by projecting the excitation dynamics to a reduced one-dimensional parameter space. Based on this analysis we show that the inward current required for an excitation to occur is largely dictated by the voltage dependence of the inward rectifier potassium current (I_{K1}), and is insensitive to the detailed properties of the sodium current. We derive an analytical expression relating the size of a stimulus and the critical current required to induce a propagating action potential (AP), and argue that this relationship determines the necessary number of cells that must undergo SCR in order to induce ectopic activity in cardiac tissue. Finally, we show that, once a focal excitation begins to propagate, its propagation characteristics, such as the conduction velocity and the critical radius for propagation, are largely determined by the sodium and gap junction currents with a substantially lesser effect due to repolarizing potassium currents. These results reveal the relationship between ion channel properties and important tissue scale processes such as excitation and propagation.

DOI: 10.1103/PhysRevE.91.042719 PACS number(s): 87.19.Hh

I. INTRODUCTION

A variety of cardiac arrhythmias are initiated by a focal excitation that propagates in heart tissue [1–5]. These excitations are typically generated by intracellular currents that are independent of the electrical activation due to the regular beating rate of the heart. An example that has been extensively studied in the literature is the case where focal excitations are caused by spontaneous calcium (Ca) release (SCR) within cardiac cells [6–11]. In this scenario, Ca is released in the cell via the formation of propagating Ca waves which then activate Ca sensitive inward currents, such as the sodium Ca exchanger, which can lead to membrane depolarization. These excitations are particularly dangerous since they disrupt the rhythmic beating of the heart, and they have a larger likelihood of inducing wavebreak and fibrillation [12–14].

The presence of inward currents in a single cell is not sufficient to induce a propagating excitation in cardiac tissue. This is because electrotonic coupling to neighboring quiescent cells will suppress membrane depolarization and therefore substantially increase the current requirements required to bring a region of tissue to threshold [1,15]. Thus, in order to induce an ectopic excitation, inward currents will have to occur within a population of cells, at roughly the same time, in order to raise that region of tissue to threshold. However, the precise requirements for this to occur are unknown since an ectopic excitation is dependent on a wide variety of factors such as ion channel gating kinetics, the gap junction coupling between cells, and the electrophysiological heterogeneities present in cardiac tissue [1,15]. Analytic approaches to determine the necessary requirements for an excitation to occur in tissue have been developed by several authors [16–20]. In particular, Idris and Biktashev [19,20] have highlighted the importance of "critical fronts" in order to demarcate the set of initial conditions which either propagate or decay. These studies make important progress in our theoretical understanding of threshold phenomenon in excitable media. However, despite this progress it is still not known how the criteria for excitation in cardiac tissue depends on the detailed properties of physiological ion currents.

In this study we apply an analytic and computational approach to determine the current requirements for a focal excitation to occur in isotropic three-dimensional (3D) heart tissue. Our analytic approach is based on the method of projected dynamics, first introduced by Neu *et al.* [18], which is applied to determine the current necessary to excite cardiac tissue. We apply this technique to an experimentally based ionic model due to Fox *et al.* [21] in order to determine how key ion channel properties dictate the threshold for excitation. Our main result is that focal excitation in heart tissue is largely dictated by the voltage dependence of the inward rectifier potassium current (I_{K1}). More precisely, we show that inward currents, due to intracellular processes such as SCR, need only raise the voltage from the resting membrane potential $V \sim -96$ mV to roughly $V \sim -70$ mV, which is the voltage at which I_{K1} attains its maximum, and not to the threshold of $V \sim -55$ mV that is required to activate the sodium current. We argue that this feature is crucial to understanding how SCR in cardiac cells can induce an ectopic excitation, and explains the propensity of Ca release abnormalities to induce dangerous focal excitations. Our approach also yields an accurate analytic expression that relates the necessary current applied to a volume of cells required to induce a propagating AP. We argue that this expression can be used to determine the number of cells undergoing SCR necessary to induce a focal excitation in cardiac tissue. Finally, we have applied the method of projected dynamics to understand the propagation of a cardiac excitation in isotropic three-dimensional (3D) cardiac tissue. We show that the sodium current plays the dominant role to determine propagation characteristics and that potassium currents play a much less important role. This is in sharp contrast to excitation properties which are dictated primarily by the voltage dependence of I_{K1}. Finally, we argue that these results can serve as a starting point to guide the development

of pharmacological interventions which seek to target specific excitation and propagation processes in the heart.

II. A SIMPLIFIED MODEL DESCRIBING CARDIAC EXCITATION

The transmembrane potential in 3D isotropic cardiac tissue is described by the cable equation

$$C_m \frac{\partial V}{\partial t} = D\,\nabla^2 V - (I_{\rm Na} + I_{\rm Ca} + I_{\rm K} + I_s)\,, \qquad (1)$$

where V is the transmembrane voltage, C_m is the cell membrane capacitance, and D is the effective diffusion coefficient of voltage in cardiac tissue. The main ion currents regulating the voltage time course are the sodium ($I_{\rm Na}$), potassium (I_K), and Ca ($I_{\rm Ca}$) currents, whereas I_s is an external stimulus current that is necessary to initiate an excitation. Under resting conditions, the membrane voltage is held at a resting potential determined primarily by the inward-rectifier potassium current I_{K1}. However, if the voltage is raised above the activation threshold of the sodium current then an action potential (AP) will occur. Under suitable conditions, if a sufficient mass of tissue is depolarized, then a propagating wave will be induced in tissue. In this study, we will consider a stimulation current that is turned on for a finite duration and applied to a spherical region of tissue. Our stimulus current has the form

$$I_s(t) = \left\{ \begin{matrix} -I & t \leqslant \tau \\ 0 & t > \tau \end{matrix} \right\}, \qquad (2)$$

for $|\boldsymbol{r}| \leqslant R$, and $I_s(t) = 0$ for $|\boldsymbol{r}| > R$, where R is the radius of tissue in which the inward current I is applied for a duration τ. Our goal is to determine the critical current $I = I_c$, for a fixed size R, such that a propagating wave is induced in isotropic 3D cardiac tissue.

In this study we will model the cell membrane numerically using an experimentally based ionic model of the ventricular myocyte due to Fox *et al.* [21]. In this model there are 13 different ionic currents which regulate the membrane potential. To understand the dynamics of excitation in this system we will first identify the essential ionic currents that are relevant to the excitation of an AP. We first note that excitation of cardiac tissue is determined primary by ionic processes that occur between the resting state at $V \sim -96$ mV and the threshold for sodium activation $V \sim -55$ mV. In this range the dominant ionic currents are $I_{\rm K1}$ and the sodium current $I_{\rm Na}$. Hence, for the purpose of computing the critical current I_c we can simplify the system by making the approximation that $I_{\rm K} \approx I_{\rm K1}$. The detailed formulation of this current in the Fox model is given by

$$I_{\rm K1}(V) = G_{\rm K1}\, K(V)\, \frac{[K^+]_o}{[K^+]_o + 13}\, (V - V_{\rm K}), \qquad (3)$$

with $K(V) = 1/\{2 + \exp[1.62(V - V_{\rm K})F/RT]\}$, where F is Faraday's constant, R is the gas constant, $[K^+]_o$ is the external potassium concentration, T is the temperature, and where $G_{\rm K1} = 2.8$ mS/μF is the channel conductance. Here $V_{\rm K} = -96$ mV is the reversal potential of $I_{\rm K1}$ which sets the resting membrane potential of the cell. In Fig. 1 we plot the voltage dependence of $I_{\rm K1}$ showing the characteristic inward rectifying feature close to $V_{\rm K}$ followed by an increase

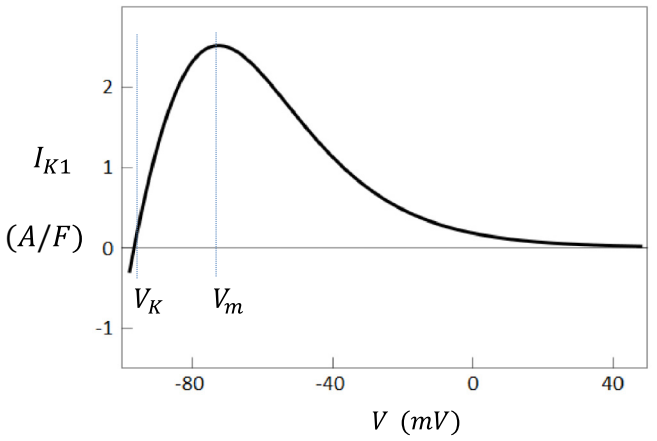

FIG. 1. (Color online) The inward rectifier potassium channel ($I_{\rm K1}$) as a function of the membrane potential V. The resting membrane potential is at $V_{\rm K} = -96.6$ mV, while the maximum of the current occurs at $V_m = -71$ mV.

in the amplitude to a global maximum at $V_m \sim -70$ mV. We note here that these features are consistent with existing experimentally based ionic models such as Shannon-Bers [22] and Luo-Rudy [23].

In most ionic models, including the Fox model used here, the sodium current has the form $I_{\rm Na} = G_{\rm Na} m^3 hj(V - V_{\rm Na})$, where $G_{\rm Na}$ is the channel conductance, where m,h, and j are the activation and inactivation gating variables, and where $V_{\rm Na} \approx 70$ mV is the reversal potential of sodium [21,23]. Inward currents due to SCR typically have a duration in the range 50–500 ms [9,10], which is substantially longer than the relaxation time of the fast sodium activation gate ($\tau_m \sim 0.1$ ms). Thus, to model excitation from the resting potential we can make the approximation that $m = m_\infty(V)$, where $m_\infty(V)$ is a sigmoid function that rises sharply from zero at the sodium activation threshold $V_c \sim -55$ mV. Similarly, the dynamics of excitation should be largely dictated by voltages between the resting state at $V_{\rm K}$ and the sodium threshold at V_c. In this regime of voltages we can make the approximations that $h = 1$ and $j = 1$ since these gates only inactivate once the voltage rises substantially above V_c. Thus, for the purposes considered here, we can simplify the sodium current to the form $I_{\rm Na} \approx G_{\rm Na} m_\infty^3\, (V - V_{\rm Na})$. Later we will validate these simplifying assumptions by a direct comparison with numerical simulations of the full Fox ionic model.

III. DYNAMICS OF EXCITATION OF AN ISOLATED CELL

In order to explore the conditions that promote an excitation to propagate in tissue it is first necessary to understand the excitation of a single cardiac cell. In this case we analyze the conditions such that a current stimulus induces the membrane voltage to rise from the resting potential to a voltage at the plateau of the AP. The voltage dynamics near the resting potential obeys an equation of the form $dV/dt = F(V,I)$, where $F(V,I) = -I_{\rm K1}(V) - I_{\rm Na}(V) - I_s(t)$. Here all currents are expressed per unit capacitance (A/F), and we consider the case where the stimulus current I is switched on at time $t = 0$ for a duration τ. In Fig. 2 we plot the total current $F(V,I)$

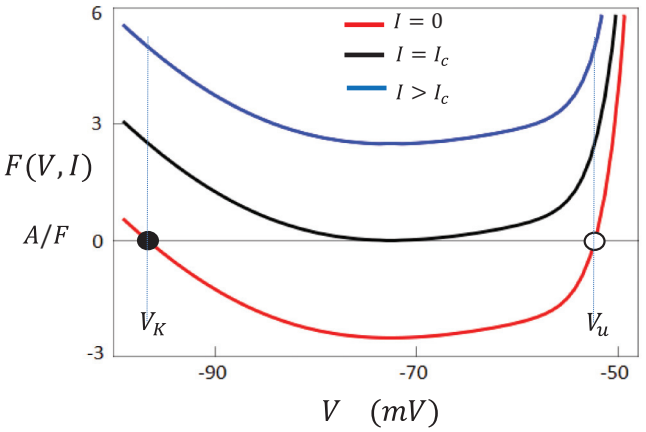

FIG. 2. (Color online) Plots of the total membrane current $F(V,I)$ for three different values of the current stimulus amplitude I. the black line indicates the case $I = I_c$, where $F(V,I_c) = 0$.

for three distinct values of the current amplitude I. In the case where $I = 0$ (red line) we note that the system has a stable fixed point at $V = V_{\rm K}$ and an unstable fixed point at $V = V_u$. Now, when the stimulus current is turned on, the function $F(V,I)$ rises (black and blue curve) so that the membrane voltage will rise accordingly since $dV/dt > 0$. Thus, the criteria for an excitation to occur is that the voltage reaches the unstable fixed point V_u before the current stimulus is turned off at time τ, since, if it does not, then the system will return to the resting potential once the stimulus is turned off at time $t = \tau$. Hence, the critical current I_c required to escape the stable fixed point is given by the condition

$$\int_{V_{\rm K}}^{V_u} \frac{1}{F\,(V,I_c)}\,dV \;= \tau. \tag{4}$$

To estimate the location of the unstable fixed point at V_u we note that the sodium activation gate is $m_\infty^3(V) \sim 0$ for $V < V_c$ and $m_\infty^3(V) \sim 1$ for $V > V_c$. Also, once the sodium current is activated it is substantially larger than the repolarizing potassium currents so that $I_{\rm Na} \gg I_{\rm K1}$. Thus we have that $F(V,0) < 0$ for $V < V_c$ and $F(V,0) > 0$ for $V > V_c$, which suggests that a good approximation for the unstable fixed point is at $V_u \approx V_c = -55$ mV. To find the critical current we evaluate Eq. (4) with $F(V,I) \approx -I_{\rm K1}(V) + I$ since $I_{\rm Na} \approx 0$ in the range $V_{\rm K} < V < V_c$. To proceed, we note that $I_{\rm K1}$ can be well approximated by a quadratic fit to Eq. (3) in the range $V_{\rm K} < V < V_c$, so that $I_{\rm K1}(V) \approx g_k(V - V_{\rm K}) - \sigma(V - V_{\rm K})^2$, where g_k and σ are fitting parameters. With this approximation, evaluation of Eq. (4) then gives the excitation criteria as an algebraic condition

$$g_k\tau = 2A(\mathrm{Tan}^{-1}(A) - \mathrm{Tan}^{-1}\{[-1 + 2(V_c - V_{\rm K})\sigma/g_k]A\}), \tag{5}$$

where $A = (-1 + 4I_c\sigma/g_k^2)^{-1/2}$. Note that this result applies only in the case where the maximum of $I_{\rm K1}$ occurs at a voltage $V_m < V_c$, which is indeed the case in the Fox model. Consequently, Eq. (5) has real solutions providing that $I_c \geqslant g_k^2/4\sigma$, which is the condition that the minimum of $F(V,I)$ is greater than zero.

To simplify this condition we will consider parameters relevant to SCR in which inward currents are applied for a duration $\tau \sim 50$–500 ms. A quadratic fit to Eq. (3) gives $g_k = 0.215\ (\mathrm{ms})^{-1}$ so that $g_k\tau \gg 1$, which requires that $1/A \sim 0$ and yields a critical current of $I_c \approx g_k^2/4\sigma$. Graphically, this solution corresponds to that current I_c that raises the total current $F(V,I_c)$ so that its minimum crosses the x axis (Fig. 2, black line). This is because in the limit this condition ensures that the dynamics of V will escape the stable fixed point at $V_{\rm K}$. Alternatively, the critical current is simply $I_c \approx I_{\rm K1}(V_m)$, where $V_m \sim -70$ mV is the voltage where $I_{\rm K1}$ attains its global maximum. Indeed, given a quadratic approximation to $I_{\rm K1}$, then the global maximum is indeed $I_{\rm K1}(V_m) = g_k^2/4\sigma$, which is consistent with Eq. (5).

In summary, we have shown that the excitation dynamics of a single cardiac cell is dictated primarily by the voltage dependence of $I_{\rm K1}$. In particular, for inward currents with a duration $\tau > 1/g_k \sim 5$ ms, which is what is expected during SCR, then the critical current is simply given by the maximum of $I_{\rm K1}$. We note here that this feature is shared by a wide range of ionic models [22,23] where the maximum of $I_{\rm K1}$, at $V_m \sim -70$ mV, occurs at a lower voltage than the sodium threshold at $V_c \sim -55$ mV. Surprisingly, in these models the sodium current does not play a role in the condition for excitation of an isolated cardiac cell.

IV. THE METHOD OF PROJECTED DYNAMICS

To analyze the dynamics of excitation in 3D isotropic cardiac tissue we will apply the method of projected dynamics first introduced by Neu *et al.* [18]. This approach relies on the observation that a partial differential equation (PDE) of the form

$$\frac{\partial v}{\partial t} = D\nabla^2 v + \; f(v) \tag{6}$$

can be written as the gradient flow of an energy functional

$$\frac{\partial v}{\partial t} = -\frac{\delta E\,[v]}{\delta v}, \tag{7}$$

where the energy is

$$E\,[v] = \int d^d\boldsymbol{r}\;[D(\nabla v)^2 + \; U(v)], \tag{8}$$

and where the effective potential is $U(v) = -\int^v f(v')dv'$. The energy functional can be evaluated by parametrizing the solution to the PDE using a function of the form $v(\boldsymbol{r},t) = v[\boldsymbol{a}(t),\boldsymbol{r}]$, where $\boldsymbol{a}(t)$ represents a vector of N parameters that specify the time evolution of the solution to the PDE. Then Eq. (7) requires that these parameters evolve according to a system of ordinary differential equations (ODEs) of the form

$$\boldsymbol{M}\frac{d\boldsymbol{a}}{dt} = -\nabla\, E, \tag{9}$$

where $\nabla_i = \partial/\partial a_i$, and where M is an $N \times N$ matrix with entries

$$M_{ij} = \int d^d\boldsymbol{r}\;\frac{\partial v}{\partial a_i}\frac{\partial v}{\partial a_j}. \tag{10}$$

Thus, by choosing a suitable ansatz for the solution of the PDE we can compute the time evolution of the system in the projected parameter space. In this study we will show that this approach can be used to attain quantitative analytic formulas for the wave excitation and propagation criteria of an experimentally based AP model.

V. DYNAMICS OF EXCITATION IN 3D TISSUE

As a starting point we will rewrite Eq. (1) using the variable $v = V - V_{\rm K}$. In this notation the threshold for sodium activation is written as $v_c = V_c - V_{\rm K}$. This gives

$$\frac{\partial v}{\partial t} = D\,\nabla^2 v - I(v), \tag{11}$$

where $I(v) = I_{\rm K1}(v) + I_{\rm Na}(v) + I_s(t)$. As in the single cell analysis, we will make the approximation that $I_{\rm K1}(v) \approx g_k v - \sigma v^2$, which is valid in the range of voltages relevant to excitation. To model the sodium current we note that $m_\infty^3(v)$ increases rapidly from zero near the threshold for sodium activation near $v \sim v_c$. To model this property we will approximate the voltage dependence of the sodium current just above v_c as a quadratic of the form $I_{\rm Na}(v) \approx -\tilde{g}_{na}\,(v - v_c)^2\,\Theta(v - v_c)$, where $\Theta(x)$ is the Heaviside step function. Here $\tilde{g}_{na}$ is a fitting parameter that is proportional to the sodium conductance $G_{\rm Na}$, and is found by fitting a quadratic to the sodium current $I_{\rm Na}(V) \approx G_{\rm Na} m_\infty^3(V)(V - V_{\rm Na})$ in the range $V_c < V < V_c + 15$ mV.

To apply projected dynamics it is necessary to choose an appropriate ansatz that will capture the main features of the solution to the PDE. In spherical coordinates we will use the function

$$v\,(r,t) = \begin{cases} s & r \leqslant R, \\ \frac{s\ R\exp[-(r-R)/l]}{r} & r > R, \end{cases} \tag{12}$$

where $l = \sqrt{D/g_k}$ is the electrotonic length. This ansatz approximates the voltage in the region $r < R$ as a constant s which parametrizes our solution, while for $r > R$ we use an exponentially decaying function that is the spherically symmetric solution of the 3D cable equation with a linear repolarizing current $I_{\rm K1}(v) \approx g_k v$. The time evolution of the voltage amplitude s, for times $t < \tau$, is then given by

$$M\frac{ds}{dt} = -\frac{dE}{ds}, \tag{13}$$

where $M = \int d^3\boldsymbol{r}\ (\partial v/\partial s)^2 = (4/3)\pi R^3 + 2\pi R^2 l$. To evaluate the energy functional given by Eq. (8) we make the approximation that the contribution due to the effective potential U is dominated by the region $r < R$ so that $\int d^3\boldsymbol{r}\ U[v(\boldsymbol{r})] \approx (4/3)\pi R^3 U(s)$, which gives $E(s) \approx D\pi R(R/l + 2)s^2 + (4/3)\pi R^3 U(s)$. Equation (13) simplifies to the form $M ds/dt = f(s,R,I)$, where $f(s,R,I) = -2D\pi R(R/l + 2)s + (4/3)\pi R^3 I(s)$. Analysis of the function $f(s,R,0)$ shows that the dynamics has a stable fixed point at $s = 0$ and an unstable fixed point at $s = s_u$. The presence of the unstable fixed point indicates that if the voltage is raised above s_u then the amplitude will increase without bound. Thus, as in the single cell case, the criteria for s to cross the threshold at s_u in the time duration τ, is given by the condition

$$\int_0^{s_u} \frac{1}{f\,(s,R,I_c)}ds\ = \frac{\tau}{M}, \tag{14}$$

which gives an analytic criterion to determine the critical current I_c as a function of the size of the stimulus R. We note here that the critical current computed using this condition only ensures that the voltage pulse will exceed the unstable fixed point s_u, but it does not ensure that the resulting AP will propagate in tissue. However, we will show later, using numerical simulations of the Fox model in 3D isotropic tissue, that the critical current I_c is always sufficient to induce wave propagation, i.e., the critical current for excitation, given by Eq. (14), is equivalent to the critical current for AP propagation.

As in the single cell case, we will solve Eq. (14) analytically for the case that is directly relevant to SCR induced excitation. In this case $g_k\tau \gg 1$ so that the critical current is the current necessary to raise $f(s,R,I)$ such that its minimum is at zero. Thus, I_c is determined by the algebraic conditions $df/ds|_{s_m} = 0$ and $f(s_m,R,\ I_c) = 0$. Here s_m is the minimum of the function $f(s,R,I)$ and is the solution of the algebraic condition

$$\begin{aligned} &3D(2 + R/l) + 2R^2[g_k - 2\sigma s_m \\ &\quad - 2\tilde{g}_{na}(s_m - v_c)\Theta(s_m - v_c)] = 0. \end{aligned} \tag{15}$$

In the case where $s_m < v_c$ we have $s_m = g_k/2\sigma + 3D(2 + R/l)/2\sigma R^2$, which holds for $R > R_c$, where R_c is the solution when $v_c = s_m$. In this regime the critical current is found by solving the algebraic condition $f(s_m,R,\ I_c) = 0$, which gives the critical current

$$I_c = \frac{g_k^2}{4\sigma}\ \Gamma^2, \tag{16}$$

where

$$\Gamma = 1 + \frac{3}{2}\left(\frac{l}{R}\right) + 3\left(\frac{l}{R}\right)^2. \tag{17}$$

However, for $R < R_c$ this solution is no longer valid since $s_m > v_c$ and the term proportional to $\tilde{g}_{na}$ in Eq. (15) must be taken into account. In this case we find that the critical current is

$$I_c = -\sigma v_c^2 + g_k v_c \Gamma + \frac{g_k^2}{4\tilde{g}_{na}}\Gamma^2, \tag{18}$$

where we have made the approximation that $\tilde{g}_{na} \gg \sigma$, which is valid in our system (see the Fig. 3 caption for parameters derived from a fitting to the Fox ionic model). Equations (16) and (18) give a full description of the excitation threshold I_c as a function of system parameters.

In order to interpret the predictions of Eq. (16)–(18) we will consider physiological parameters derived from the Fox ionic model. First, we note that the critical current is a function of the dimensionless parameter l/R where $l = \sqrt{D/g_k}$ is the electrotonic length. In this study we use a standard value of $D = 5 \times 10^{-3}$cm^2/ms and $g_k = 0.215$ ms^{-1}, which gives $l \sim 0.15$ cm. So that, according to Eq. (17), the critical current begins to rise substantially when $R < l$. Now, in the limit $R > l$, we find that the critical current decreases to the single cell limit where $I_c \sim I_{\rm K1}(V_m) \sim 2.6$ A/F. On the other hand, in

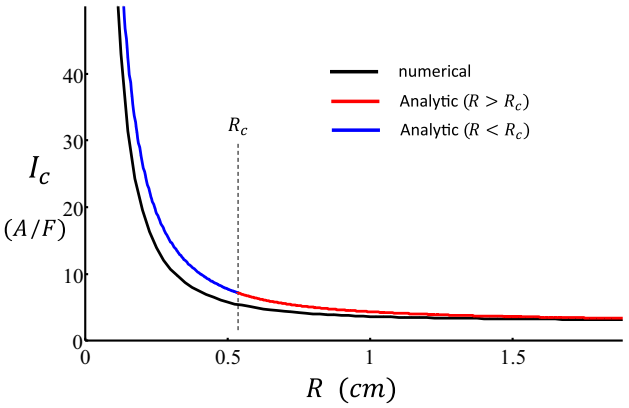

FIG. 3. (Color online) The critical current I_c for AP propagation for a spherically symmetric stimulus of radius R. Numerical prediction (black line) and analytic prediction for $R > R_c$ (red) and $R \leqslant R_c$ (blue). A fitting of I_{K1} and I_{Na} in the voltage range $-95 < V < -40$ mV, yields parameters $g_k = 0.215$ $(\text{ms})^{-1}$, $\sigma = 0.0045$ $(\text{mV ms})^{-1}$, $v_c = -55$ mV, $\tilde{g}_{na} \sim 1.0$ $(\text{mV ms})^{-1}$, and where we used $D = 5 \times 10^{-3}$ (cm^2/ms).

the case where $R < R_c$ the critical current is given by Eq. (18) and exhibits a dependence on properties of I_{Na} such as the conductance $\tilde{g}_{na}$ and the threshold for activation v_c. However, examination of the terms reveals that $g_k^2/4\tilde{g}_{na} \sim 0.01$ so that the third term is substantially smaller than the first two terms. This result indicates that the critical current in this regime is mainly sensitive to the sodium current via the threshold for activation v_c.

To confirm our analytic predictions for the critical curve we have solved the cable equation in 3D spherical coordinates using a standard finite difference scheme. All ionic currents are taken directly from the Fox model with all ionic currents included, and we have taken the effective diffusion coefficient of voltage to be $D = 5 \times 10^{-3}\text{cm}^2/\text{ms}$. Here we consider only spherically symmetric solutions and solve the radial equation with a space step of $\Delta r = 5.0 \times 10^{-3}\text{cm}$ and time step of 2.5 μs. Our current pulse is applied in a region $r \leqslant R$ for a duration $\tau = 50$ ms, and initial conditions are chosen so that the tissue is at the resting membrane potential (~ -96 mV). To generate the critical curve we increase the stimulus amplitude I in small increments until the voltage at $r = 0$ rises rapidly from the resting state at -96 mV to a value above 20 mV. A plot of the threshold I_c vs the stimulus radius R then gives the critical curve for excitation. In Fig. 3 we have plotted the critical curve for the full Fox model, which is in excellent agreement with the analytic prediction given by Eqs. (16) and (18) above. In both cases we find that as the region of excitation R decreases the critical current increases substantially. The analytic prediction indicates that this increase occurs near the electrotonic length $l \sim 0.15$ cm, which is consistent with the numerical predictions. We note here that we find similar agreement between the approximate and numerical predictions for a wide range of D and g_k values, and that the critical current always increases when the stimulus size is near $l = \sqrt{D/g_k}$.

The critical current for excitation given by Eqs. (16)–(18) determines an approximate condition such that an applied current will induce the voltage in that region to rise above the threshold for excitation. However, this condition is itself not sufficient to ensure propagation of an AP. To determine the criteria for propagation it is necessary to determine the critical current after which an AP will propagate to $r \gg R$. To compute the critical current for propagation numerically we again increase I in small increments and then record the critical current I_p when the voltage at $r = 2$ cm exceeds $V = 20$ mV, within a 50 ms interval after the stimulus has been turned off. Our numerical simulation results reveal that $I_p \approx I_c$ so that for the Fox ionic model the critical curve for excitation serves as an excellent approximation for the critical curve for propagation.

Our analytical approximation for the critical curve gives a quantitative estimate of the critical current for excitation of a physiologically detailed ionic model. Here we discuss the limitations of the approximation and the source of the deviation between the analytic and numerical results. Recall that an important feature of our approximation was the ansatz for voltage shape [Eq. (12)], which determined the parameter space of the projected dynamics. While this functional form captured the essential features of the excitation process, it overly simplified the spatial dependence of the solutions. In particular, we approximated the voltage to be constant for $r \leqslant R$ while the exact solution displays a more complex space dependence. Hence, the reduced parameter space used here neglects spatial information which contributes to the observed difference between the theory and simulation results. However, we stress here that a more accurate ansatz will have to be represented by more parameters, and will thus yield a projected dynamics that will be substantially more difficult to analyze. In fact, it is not clear that the critical curve can be found in higher dimensions since this will correspond to an unstable manifold, for which a concise analytic form is in general difficult to determine. Hence, the advantage of our approach is that it is analytically tractable, yet captures the main features of the parameter dependence of the critical curve. A second source of the discrepancy is that we have approximated the nucleation dynamics by assuming that the time scale for inactivation of the sodium current is much slower than the excitation process. However, these time dependent processes in the physiologically detailed ionic model do lead to small corrections to the critical curve, and these effects are not captured by the method of projected dynamics. Again, we stress that despite these limitations our approach yields simple quantitative expressions that capture the essential features of the critical current for excitation.

VI. APPLICATION OF PROJECTED DYNAMICS TO DETERMINE PROPERTIES OF AP PROPAGATION

In this paper we have shown that the method of projected dynamics gives an excellent description for the critical current for propagation. However, this analysis does not shed light on the characteristics of wave propagation once it has been excited. Here we will apply projected dynamics to determine the propagation velocity and the critical radius for propagation for a spherically symmetric AP excitation. Our aim in this analysis is twofold. First, our analysis will shed light on the role of specific ion currents that determine important

properties of wave propagation in tissue, and second, we will demonstrate that projected dynamics serves as a powerful tool to derive quantitative analytic expressions that describes propagation characteristics of an experimentally based ionic model.

As a starting point we will consider the evolution of a spherically symmetric AP pulse with an interface at $r = R$ so that $V(r < R) = V_p$ and $V(r > R) = V_{\rm K}$. Here V_p is the voltage during the AP, and $V_{\rm K}$ is the resting membrane potential. To apply the method of projected dynamics we will again approximate these currents with simple functional forms that capture the main current contributions in the relevant voltage range. In particular we will make the approximation that $m^3 = m^3_\infty(V) = \Theta(V - V_c)$. This approximation is valid for our purposes here since $m^3 \sim 0$ or 1 for a large fraction of the voltage range at the excitation front. Also, we make the approximation that the inactivation gate is turned off once the voltage reaches the plateau potential V_p, so that we have $h = h_\infty(V) = 1 - \Theta(V - V_p)$. Finally, we assume that the slow activation gate is given by $j = 1$ for the region of cells near the AP front. Thus, we will approximate the sodium current as $I_{\rm Na} \approx g_{na}(V - V_{\rm Na})\Theta(V - V_c)\ [1 - \Theta(V - V_p)]$. To model $I_{\rm K1}$ we will use the approximation that $I_{\rm K1} \approx g_k[1 - \Theta(V - V_c)](V - V_{\rm K})$, so that the $I_{\rm K1}$ current is turned off when $V > V_c$. This approximation is justified by the fact that above V_c the inward current is dominated by $I_{\rm Na}$ so that the contribution of $I_{\rm K1}$ is negligible. Later we will justify the validity of these simplifications via a direct comparison to the Fox ionic model. To proceed, the effective potential energy defined in Eq. (8) is given by

$$U(V) = \begin{cases} (g_k/2)\,(V - V_{\rm K})^2 & V_{\rm K} \leqslant V \leqslant V_c \\ (g_k/2)\,(V_c - V_{\rm K})^2 - (g_{na}/2)\ ((V_{\rm Na} - V_c)^2 - (V_{\rm Na} - V)^2) & V_c < V \leqslant V_p \end{cases}. \tag{19}$$

To apply projected dynamics we will consider a propagating pulse that is approximated as a piecewise linear function along the radial direction, as illustrated in Fig. 4. We model the excited phase by a constant voltage V_p for a radial distance R, and use a straight line interface of width l to connect V_p to the resting membrane potential at V_K. Thus, in the interface region, the voltage profile will have the form $V(r) = V_p - (V_p - V_{\rm K})r/l$. In this approach the motion of the wave front is projected into the two-dimensional subspace of the interface width l and the pulse radius R.

To evaluate the energy of our spatial profile we assume that the interface width l is sharp so that $l \ll R$. The total energy can then be approximated as

$$E(R,l) \approx \tfrac{4}{3}\,\pi R^3\ U(V_p) + 4\pi R^2 W, \tag{20}$$

where the interface energy is given by

$$W = \frac{D}{2}\frac{(V_p - V_{\rm K})^2}{l} + \Delta U\ l, \tag{21}$$

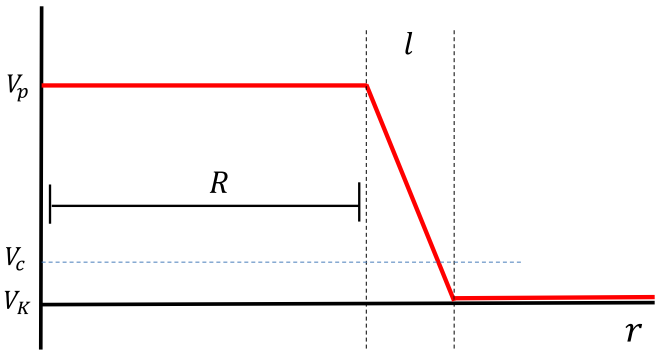

FIG. 4. (Color online) Illustration of the radial profile of a linearly piecewise function used to approximate the shape of an AP front. Application of projected dynamics yields ODEs governing the time evolution of the front position R, and the interface width l.

where $\Delta U = U_{\rm int} - U(V_p)$, and where

$$U_{\rm int} = \frac{1}{V_{pk}}\left[\frac{g_k V_{ck}^3}{6} + \frac{g_k V_{ck}^2 V_{pc}}{2} - \frac{g_{na}}{6}\ V_{pc}^2(V_{np} - 2V_{nc})\right], \tag{22}$$

with $V_{ck} = V_c - V_{\rm K}$, $V_{pc} = V_p - V_c$, $V_{np} = V_{\rm Na} - V_p$, $V_{nc} = V_{\rm Na} - V_c$. The projected dynamics is then given by the 2×2 matrix equation

$$\boldsymbol{M}\,\frac{d}{dt}\begin{pmatrix} l \\ R \end{pmatrix} = -\begin{pmatrix} \frac{\partial E}{dl} \\ \frac{\partial E}{\partial R} \end{pmatrix}, \tag{23}$$

where the matrix elements are $M_{11} = \int_0^\infty dr\, 4\pi r^2\,(\partial V/\partial l)^2$, $M_{22} = \int_0^\infty dr\, 4\pi r^2 (\partial V/\partial R)^2$, and $M_{12} = M_{21} = \int_0^\infty dr\, 4\pi r^2 (\partial V/\partial l)(\partial V/\partial R)$. We note that for our piecewise function $V(r)$ derivatives with respect to the parameters l and R are nonzero only at the interface. Thus, $r \sim R$ where the integrands are nonzero and $M_{11} \approx 4\pi R^2 \int_0^\infty (\partial V/\partial l)^2 dr$, $M_{22} \approx 4\pi R^2 \int_0^\infty (\partial V/\partial R)^2 dr$, and $M_{12} \approx 4\pi R^2 \int_0^\infty (\partial V/\partial l)(\partial V/\partial R)\ dr$. We note that $\partial V/\partial l$ is antisymmetric around the position of the interface R, so that in the thin interface limit $M_{12} \sim 0$. Time evolution of the interface width is then governed by $dl/dt = -(\partial W/\partial l)/M_{11}$, so that the steady state interface width is given by $l^* = \sqrt{D/2\Delta U}$. The radial equation $dR/dt = -(\partial E/\partial R)/M_{22}$ can be simplified to the form

$$\frac{dR}{dt} = v\left(1 - \frac{R_n}{R}\right), \tag{24}$$

which predicts that a spherical pulse of radius R will propagate providing that $R > R_n$, where

$$R_n = -2\sqrt{2D\Delta U}\,\frac{V_{pk}}{U(V_p)}, \tag{25}$$

with a steady state conduction velocity (CV) given by

$$v\ = -\sqrt{\frac{D}{2\Delta U}}\,\frac{U(V_p)}{V_{pk}}, \tag{26}$$

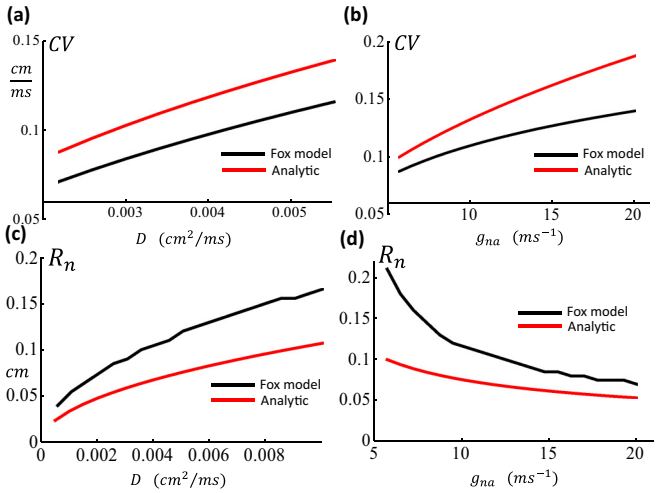

FIG. 5. (Color online) Application of projected dynamics to determine the parameter dependence of propagation characteristics of a spherical AP pulse. (a) and (b) CV vs D and g_{na}. (c) and (d) The critical radius R_n vs D and g_{na}. When not varied we fix $D = 5 \times 10^{-3}$ (cm^2/ms), and $g_{na} = 10$ (ms)$^{-1}$.

which is valid in the limit $R \to \infty$. These expressions give an analytic description of the key properties of a propagating spherical pulse in cardiac tissue.

To extract the physical interpretation of Eqs. (25) and (26) we again apply physiological parameters to determine the leading order behavior relevant to cardiac tissue. Inspection of the Fox ionic model gives $g_{na} = 10$ (ms)$^{-1}$ so that $g_k/g_{na} \sim 0.02$, and $U_{\rm int}$ and $U(V_p)$ are dominated by terms proportional to g_{na}. Keeping only the dominant terms gives $U(V_p) \approx -g_{na}V_{nc}^2/2$ and $\Delta U \approx g_{na}V_{nc}^2/2$, which yields $v \approx \sqrt{g_{na}D}\,(V_{nc}/2V_{pk})$ and $R_n \approx 4\sqrt{D/g_{na}}\,(V_{pk}/V_{nc})$. This result indicates that AP propagation is largely dictated by $I_{\rm Na}$ and the gap junction conductance, which determines the voltage diffusion coefficient D. Here $I_{\rm K1}$ plays a role in the leading order behavior only by setting the resting membrane potential $V_{\rm K}$. However, the detailed properties of this channel, such as the conductance and voltage dependence, play a minor role in the AP propagation characteristics.

In order to check the validity of Eqs. (25) and (26) we have numerically simulated the Fox ionic model to compute the propagation characteristics of a spherical AP pulse. As a starting point we computed the CV by initiating a spherical pulse and measuring the wave front velocity far from the point of stimulation. In Figs. 5(a) and 5(b) we plot the CV as a function of both the sodium current conductance and the effective diffusion coefficient of voltage in cardiac tissue. On the same graph we show the predictions due to Eq. (26) showing semiquantitative agreement. Here we note that the Fox ionic model is developed for the canine ventricular myocyte. For the range of diffusion constants simulated we see that the Fox model predicts a CV in the range ~0.05–0.1 cm/ms, while our analytic approximation overestimates the CV in the range 0.08–0.15 cm/ms. Here we point out that experimental measurements of the CV in the canine heart have been performed in classic experiments, and a wide range of values have been reported depending upon the location in the heart [24–26]. For example, in the ventricle the CV is measured in the range 0.045–0.075 cm/ms in the longitudinal direction, while in Purkinje fibers the CV is substantially more and is roughly ~0.2 cm/ms [26]. Also, in the His bundle branch the CV was measured in the range 0.13–0.17 cm/ms [27]. Thus, our analysis does yield a semi quantitative range of CVs, and should be a good starting point to analyze the functional dependence of CV on physiological parameters.

Using projected dynamics we have also computed the critical radius for propagation by choosing initial conditions so that $V(r) = V_p = 1$ mV within a radius of $r < R$ and $V(r) = V_{\rm K} = -96$ mV for $r > R$. We then increased the initial radius R until a pulse propagates to $r \gg R$. Again, we find that the analytic predictions due to Eq. (25) gives a semiquantitative description of the critical radius for propagation. These results show that the method of projected dynamics can be used to derive analytic expressions that can be compared to an experimentally based ionic model. Insights from this analysis will be discussed in detail in the discussion section.

VII. DISCUSSION

The physiological parameters that govern the excitation of an AP pulse. In this paper we have applied the method of projected dynamics to derive the relationship between the critical current and the size of the stimulus. Our analytic results, given by Eqs. (16)–(18), are in excellent agreement with numerical simulations of the Fox ionic model. These results indicate that for $R > l \sim 0.15$ cm the critical current is well approximated by the value of I_{K1} at its global maximum. Existing ionic models of $I_{\rm K1}$ give $I_c \sim 2.6$ A/F, which is the minimum inward current due to SCR that can induce a cardiac excitation in tissue. More precisely, during SCR the stimulus current will be generated by the sodium-calcium exchanger, which is activated by the release of Ca into the cell. To estimate this current we rely on the experimental measurements of Schlotthauer *et al.* [28] who found that the total charge pumped out of the cell during Ca release from the sarcoplasmic reticulum (SR) in rabbit myocytes is roughly ~1 C/F. Assuming this charge is pumped out of the cell in roughly 100–500 ms, this gives a current of $I_{\rm NaCa} \sim 2$–10 A/F. Thus, if SCR occurs in a region of cells with $R > l$, and is synchronized over a time scale ~100 ms, then sufficient current can be induced to generate a propagating excitation. Here we stress the observation that in this regime the critical current for excitation is independent of the sodium current $I_{\rm Na}$. This is because the maximum of $I_{\rm K1}$ occurs at a voltage that is ~15 mV lower than the sodium activation threshold at $V_c \sim -55$ mV. Thus, while the activation of the sodium channel plays an important role to drive an excitation, the current requirements to reach the excitation threshold is dictated entirely by the voltage dependence of $I_{\rm K1}$. On the other hand, for stimulus regions of size $R < l$ we find that the critical current for excitation increases as a power of the dimensionless number l/R. This is because at the electrotonic length scale l, neighboring quiescent cells more effectively suppress membrane depolarization due to inward currents generated inside the volume of radius R. Our analysis reveals

further that for $R < R_c$ the critical current for excitation attains a dependence on the sodium current [Eq. (18)] via a dependence on the sodium activation threshold. Thus, our analysis suggests that excitation is dependent on the sodium threshold, but is likely insensitive to other properties of the sodium channel.

The number of cells required to undergo SCR in order to induce an ectopic excitation. In this paper we have found that the critical current increases rapidly with decreasing stimulus size R. Here we will argue that this length scale dictates the typical number of cells that will induce a focal excitation in cardiac tissue. We first note that SCR is a stochastic process that must occur in an ensemble of cells in tissue in order for that region to reach threshold. Now, if we denote the probability that a single cell undergoes SCR in a given time duration, say the diastolic interval (DI), as p, then the probability $P(n)$ that a region of n cells undergoes SCR at roughly the same time is just $P(n) \sim p^n$, since each SCR event is independent. Thus, $P(n)$ should decrease exponentially with the number of cells n required to fire. This result implies that excitations will occur, with overwhelming likelihood, in the smallest volume of tissue such that the inward current will just exceed I_c. Thus, the length scale of excitation should be well approximated by the intersection of the critical current curve (Fig. 3) and the inward current generated by SCR via the I_{NaCa} current. For example if we take $I_{\mathrm{NaCa}} \sim 10$ A/F, which is on the higher range of SCR according to [28] then the minimum size of tissue to induce an excitation is $R_e \sim 0.3$ cm. Given that the size of a cell is roughly $l_{\mathrm{cell}} \sim 100$ μm, the number of cells required to induce SCR in 3D cardiac tissue is $n \sim (R_e/l_{\mathrm{cell}})^3 \sim 27\,000$. Now, for Purkinje fibers, which are effectively one-dimensional strands of tissue, the number of cells within an electrotonic length is roughly $n \sim R_e/l_{\mathrm{cell}} \sim 30$. Thus, given that SCR is a stochastic event the likelihood of SCR originating from the Purkinje system is substantially larger than in 3D connected tissue. This result is consistent with experimental findings indicating that ectopic activity in mice suffering from catecholaminergic polymorphic ventricular tachycardia (CPVT), a lethal familial disease characterized by a higher likelihood of SCR, originate from the Purkinje system [29].

I_{K1} dictates excitation while I_{Na} determines propagation. In this paper we have applied the method of projected dynamics to analyze both excitation and propagation properties of an AP pulse. This approach gave quantitative analytic expressions for the excitation criteria, the conduction velocity, and also the critical radius for an AP pulse to propagate. Our results reveal that I_{K1} is the dominant ion current that determines the criteria for excitation from the resting membrane potential. On the other hand, once an AP is nucleated, I_{Na} and the gap junction conductance dictate the main properties of AP propagation. In fact, our analysis predicts that the conductance of I_{K1} only enters via the ratio g_k/g_{na} which is small in all the existing ionic model formulations. This is in sharp contrast to Eq. (18) where the sodium conductance contribution enters via the ratio $g_k^2/\tilde{g}_{na}$ which is also small compared to the other terms. These observations highlight the relative importance of I_{K1} and I_{Na} in distinct excitation and propagation processes in cardiac tissue. We argue here that our results provide a guide to possible pharmacological interventions that seek to target cardiac arrhythmias. In particular, our results suggest that any pharmacologic intervention that seeks to suppress ectopic activity must target the voltage dependence of I_{K1}, while interventions that modulate I_{Na} will have little or no effect. More precisely we point out that it is the voltage at which I_{K1} attains its maximum that plays an important role. Hence, this work identifies the precise feature of I_{K1} that must be modified in order to more efficiently suppress the formation of ectopic activity. On the other hand, interventions that seek to modify propagation characteristics such as conduction velocity must target detailed features of I_{Na}. Our analytic results indicate that I_{K1} influences wave propagation behavior only via the resting potential V_{K}, but that detailed properties of this current play a relatively minor role in propagation characteristics. Thus, our findings provide a framework to assess how specific ion currents influence the key physiological processes that determine cardiac excitation and propagation.

ACKNOWLEDGMENT

This work was supported by the National Heart, Lung, and Blood Institute Grant RO1HL119095.

[1] W. Chen, M. Asfaw, and Y. Shiferaw, Biophys. J. **102**, 461 (2012).
[2] R. P. Katra and K. R. Laurita, Circ. Res. **96**, 535 (2005).
[3] K. R. Laurita and R. P. Katra, J. Cardiovasc. Electrophys. **16**, 418 (2005).
[4] S. Kimura, J. S. Cameron, P. L. Kozlovskis, A. L. Bassett, and R. J. Myerburg, Circulation **70**, 1074 (1984).
[5] C. T. January and H. A. Fozzard, Pharmacol. Rev. **40**, 219 (1988).
[6] J. A. Wasserstrom *et al.*, Circ. Res. **107**, 1117 (2010).
[7] W. Chen, G. Aistrup, J. A. Wasserstrom, and Y. Shiferaw, Am. J. Physiol. Heart Circ. Physiol. **300**, H1794 (2011).
[8] G. S. Hoeker, R. P. Katra, L. D. Wilson, B. N. Plummer, and K. R. Laurita, Am. J. Physiol. Heart Circ. Physiol. **297**, H1235 (2009).
[9] B. D. Stuyvers, P. A. Boyden, and H. E. ter Keurs, Circ. Res. **86**, 1016 (2000).
[10] H. Cheng and W. J. Lederer, Physiol. Rev. **88**, 1491 (2008).
[11] H. E. Ter Keurs and P. A. Boyden, Physiol. Rev. **87**, 457 (2007).
[12] M. Haissaguerre *et al.*, New England J. Med. **339**, 659 (1998).
[13] S. M. Pogwizd, J. P. McKenzie, and M. E. Cain, Circulation **98**, 2404 (1998).
[14] J. N. Weiss, Z. Qu, P. S. Chen, S. F. Lin, H. S. Karagueuzian, H. Hayashi, A. Garfinkel, and A. Karma, Circulation **112**, 1232 (2005).
[15] Y. Xie, D. Sato, A. Garfinkel, Z. Qu, and J. N. Weiss, Biophys. J. **99**, 1408 (2010).
[16] D. Noble, J. Physiol. **226**, 573 (1972).
[17] W. A. H. Rushton, Proc. R. Soc. London (Biol.) **124**, 210 (1937).

[18] J. C. Neu, S. Preissig, and W. Krassowska, Physica D: Nonlinear Phenom. **102**, 285 (1997).
[19] I. Idris and V. N. Biktashev, Phys. Rev. Lett. **101**, 244101 (2008).
[20] I. Idris and V. N. Biktashev, Phys. Rev. E **76**, 021906 (2007).
[21] J. J. Fox, J. L. McHarg, and R. F. Gilmour, Jr., Am. J. Physiol. Heart Circ. Physiol. **282**, H516 (2002).
[22] T. R. Shannon, F. Wang, J. Puglisi, C. Weber, and D. M. Bers, Biophys. J. **87**, 3351 (2004).
[23] C. H. Luo and Y. Rudy, Circ. Res. **74**, 1071 (1994).
[24] M. S. Spach, J. M. Kootsey, and J. D. Sloan, Circ. Res. **51**, 347 (1982).
[25] J. Kupersmith, E. Krongrad, and A. L. Waldo, Circulation **47**, 776 (1973).
[26] T. Sano, N. Takayama, and T. Shimamoto, Circ. Res. **7**, 262 (1959).
[27] A. L. Waldo, E. Krongrad, J. Kupersmith, O. R. Levine, F. O. Bowman, Jr., and B. F. Hoffman, Circulation **53**, 176 (1976).
[28] K. Schlotthauer and D. M. Bers, Circ. Res. **87**, 774 (2000).
[29] M. Cerrone *et al.*, Circ. Res. **101**, 1039 (2007).